Physical Aspects for the W7-X Divertor Design

H. Renner, D. Sharma, J. Kisslinger[1] , J. Boscary, H. Grote, R. Schneider
Max-Planck-Institut für Plasmaphysik, IPP-Euratom Association
Teilinstitut Greifswald, Wendelsteinstr. 1, D-17491 Greifswald, Germany
[1]Max-Planck-Institut für Plasmaphysik, IPP-Euratom Association
Boltzmannstr. 2, D-85748 Garching, Germany

Abstract

The stellarator Wendelstein 7-X is a large "advanced stellarator" of the HELIAS-type (R=5.5 m, a=0.55 m, B_o=3 T with super conducting coils, five periods, moderate shear and variable rotational transform $5/6 \leq \iota \leq 5/4$ at the boundary) with the aim to demonstrate the reactor potential of this stellarator line at steady-state operation close to fusion relevant parameters. An „open divertor“ was chosen as a first step of divertor development for the extended magnetic and plasma parameter range. The geometry and the specifications of the in-vessel components reflecting the 3D topology of the boundary are defined in accordance with the operation range and results of various theoretical studies.

1. INTRODUCTION

The advanced **HELIAS** 3D magnetic configuration can be generated by modular twisted coils, which create both the required helical and toroidal current components. Favourable magnetic parameters can be reached including appropriate Fourier components in the field composition. The architecture of the magnetic configuration and the design of modular coils has been chosen on the basis of the optimisation principles [1,2,3].

2. CHARACTERISTICS OF THE DEVICE

2.1 Magnetic configuration of W7-X

W7-X is a **HELI**cal **A**dvanced **S**tellarator (HELIAS) with strongly varying plasma cross section, 5 field periods and low shear. The cross-section of the magnetic surfaces in W7-X changes periodically as one proceeds in toroidal direction, with poloidal symmetry planes showing either a bean-shaped or a triangular shaped contour. Due to the resonances of sideband Fourier components of the radial B spectrum with the local values of the rotational transform and the low shear situation of the W7-X configuration natural islands are generated. The LCMS of the confinement area is either defined by the inner separatrix of a natural island chain which is intersected by target plates or by an ergodised outer layer with remnants of O- and X-points of related islands. Unlike in tokamak divertors, the X-lines in island divertors are helical, with the pitch depending on the resonant rotational transform of the island chain. For the standard magnetic configuration ($\iota = 1 = 5/5$ at the boundary), five toroidally closed helical X-lines are present. In the case of extended islands, the positioning of divertor elements along the helical edge (areas with the strongest poloidal curvature of the magnetic surfaces) allows to concentrate the plasma flow on target plates and to uncouple the plasma core from the wall completely. The combination of the modular coil set with planar ancillary coils provides possibilities to change the magnetic parameters: rotational transform, shear, ripple etc.(Fig.1).
Adapted to the 3D topography of the W7-X configuration, the island divertor concept seems to be a special solution for efficient divertor operation in a HELIAS configuration [4, 5].

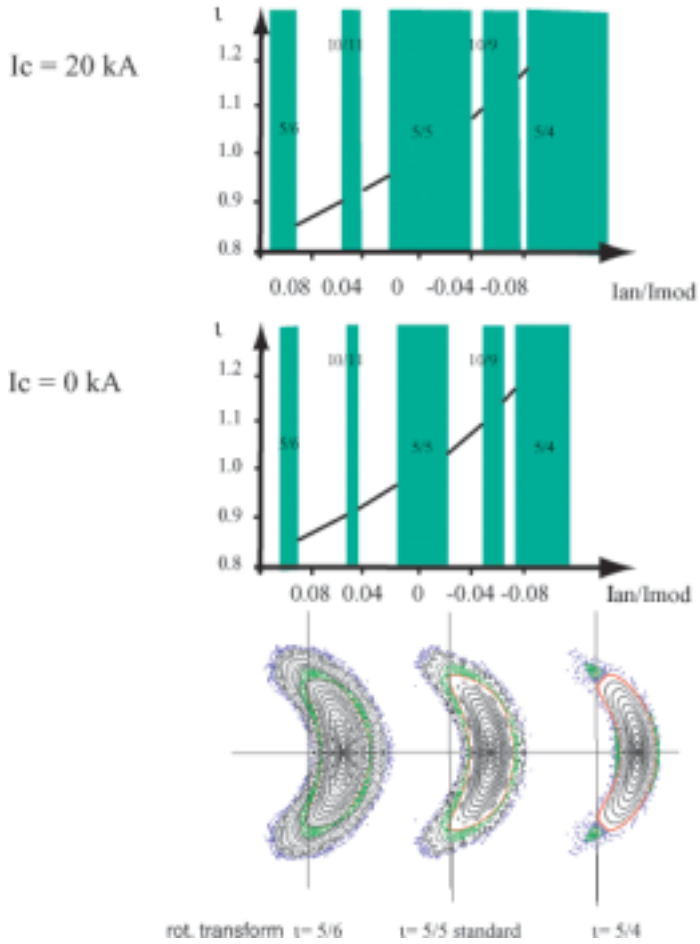

Fig. 1:
Magnetic parameter range for W7-X:
By the superposition of toroidal field components supplying the ancillary coils the rotational transform at the boundary will be modified. With the appearance of islands divertor operation at particular boundary symmetry can be achieved. The island chains related to 5/6, 5/5 and 5/4 are of particular interest. At the „white area" with the current ratio I_{AN}/I_{MOD} limiter operation, the LCMS determined by the target contact, will be achieved.
The application of the control coil fields extents the divertor operation conditions (green areas) by the variation of the island size and stochasticity at the boundary.
The for W7-X characteristic mode of operation at rotational transform ι = 5/6, 5/5=1 and 5/4 the vacuum configuration is illustrated by the correlated magnetic surface plots (φ=0°, bean shaped cross-section) at the lower part of the figure. The LCMS is indicated by red colour, the island area by green colour.

2.1.1. Control coils

The main features of the control coils are: To control the connection length L_c and modify the distance between target plates and separatrix by changing the island size at the boundary. This system consists of two current loops in each field period inside the vacuum vessel. These normal conducting saddle-shaped coils with dimensions of about 0.3*1.8 m^2 are located behind the target plates. Further application of the control coil system is the compensation of symmetry-breaking error fields, e.g. due to small construction inaccuracies of the device. Error field compensation is achieved by an individual choice of current in each control coil.
If the diffusive broadening of deposition areas on the targets is too small, the control coils can be used to sweep the strike points on the targets to prevent excessive power load. Currents of 10 kA shift the strike points on the target plates about 5 cm poloidally. A sweeping effect is introduced when energising the coils by AC currents, the transient magnetic field of the control coils oscillates the strike points on the target plates.

2.1.2 Quality of the magnetic configuration

The realisation of topology of the chosen magnetic configuration and the positioning of the divertor units in space will decide about the quality of the divertor operation. In this respect careful control of the dimensions of the coils, precise arrangement and assembling of the coil system, minimisation of stray fields, on the one side, and accurate adjustment of the in-vessel components are essential. Field errors, especially symmetry breaking faults can be tolerated only up to a level of $\Delta B/B = 10^{-4}$. The generation of islands at any periodicity, modification of the islands, being necessary for divertor operation and enhancement of the stochasticity will be severe perturbations. The standard case, ι=5/5=1, with 5 islands at the boundary is particularly sensitive – an 1/1 island could dominate the magnetic structure and interaction

with the divertor units leading to excessive asymmetric power loads [6]. Systematic errors can be allowed with higher tolerances. Therefore, manufacturing in half field and field periods before the final completion of the total system is a guideline for the engineering.
Special efforts of the engineering during assembling and a robust flexible design of the divertor components are requirements for the success of the experiment W7-X.

2.2 Heating systems

In stage I, the experiments will concentrate on the steady-state issue and the related questions on confinement, particle and power exhaust, and control. ECRH will be the main heating system with 10 MW power because of its cw capability and the uncoupling from particle fuelling. ECRH proved its capability for plasma start-up and heating towards the envisaged parameters. NBI and ICRH will be available with somewhat lower power to increase the experimental flexibility. Stage II will concentrate on high β physics and NBI will be upgraded towards 20 MW, which is necessary to reach the β limits at reduced magnetic field and high density [4].

2.3 Stationary operation

To achieve reliable and relevant data for the further improvement of the stellarator concept quasi-stationary operating conditions are mandatory. The macroscopic MHD time to establish an equilibrium of the confinement - in respect of bootstrap current, current density distribution, etc. - is about 10 seconds, whereas the time constants related to the gas inventory of the wall and impurity flux from the plasma-wall interaction are in the order of minutes.
The specification and integration of divertor components has to reflect these needs (Fig. 2).

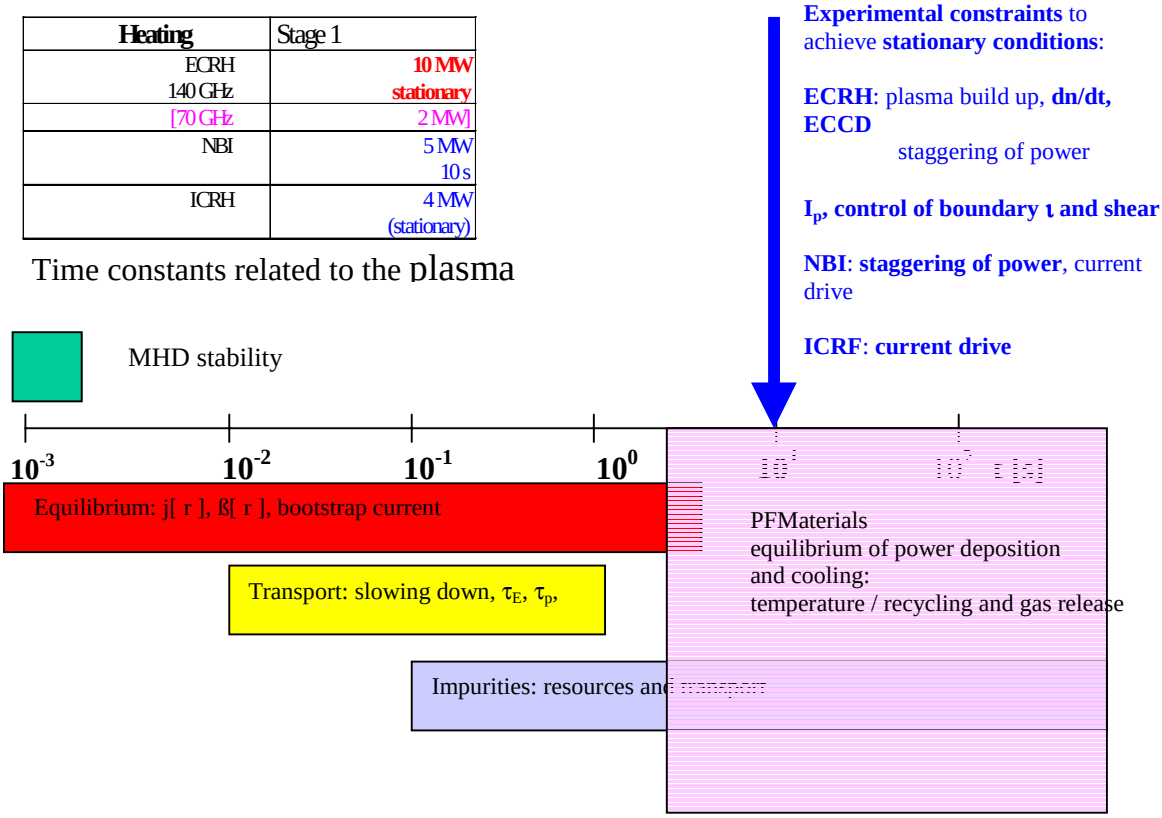

Fig. 2: Time constants related to W7-X experiments. The time needed for plasma processing to establish stationary conditions for the experimental conditions t is typically 10 s.

For safe operation of the divertor components operational diagnostics, thermography, thermometry, flow control, measurements of thermo-currents, will be installed. Supplementary sophisticated diagnostics will be used to measure the plasma parameters of the boundary and at the interacting areas.

3. DIVERTOR MODELLING

An "open divertor" system [4, 7] was chosen in a first approach to achieve effective power and particle exhaust in the wide envisaged magnetic parameter range. At the beginning of the design the geometry and specifications of the divertor was based on simplified models and analogies to tokamaks. The main input data for the geometrical and technical specification of the divertor have been provided by 3D field line tracing [8]. In combination with simulation of perpendicular transport (a typical transport coefficient is 1m²/s, values up to 10 m²/s were investigated) by Monte-Carlo code the power load was estimated. Typical connection length L_c at the boundary are between 300 m and 15 m. There is a clear correlation between field line length and its minimum distances from the LCMS – the field line length decreases as the distance from the LCMS increases.

Simplified 3D SOL models were evaluated to get information about the temperature and density distribution. For this, the 3D flux topology was combined with 1D fluid models. This method has benefits from the ordering of the open flux bundles outside the separatrix region [9].

A new code, MFBE [10], was developed for the computation of finite-β magnetic fields. It evaluates magnetic fields by using the results of the NEMEC free-boundary finite-β equilibrium code. Fig. 3 shows the deposition pattern on the chosen target plates for the vacuum case $<\beta> = 0$ and for $<\beta> = 4\%$. In both cases, the divertor plates intersect the macroscopic "islands" because the fixed points of the 5/5 islands hardly change their positions. The plasma boundaries of the finite-β equilibria lie inside the LCMS of the vacuum field, while the edge region ergodizes and the width of the islands normally extends with increasing β.

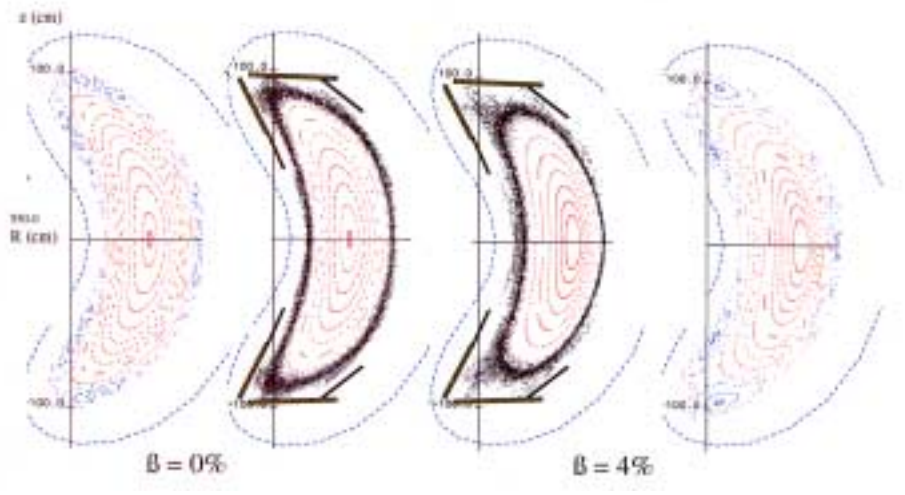

Fig 3:
Poincaré plot of the symmetric bean-shaped cross-section for the vacuum case $<\beta> = 0$ (left) and $<\beta> = 0.04$ (right). The thick bars show the target plates, whereas the thin ones mark the baffle plates. The centre plots present the corresponding results of transport simulation by field line diffusion. Standard case.

In order to quantify the stochasticity, bundles of field lines forming flux tubes are traced in this region taking into account the geometry of the plasma-facing components, i.e., the divertor, target, baffle, side plates and the first wall [11].

The multi-fluid code B2 [12] was adapted to describe the SOL parameters. Since B2 is a 2D code the geometry of the boundary was averaged (distances) and integrated (areas and volumes) in the toroidal direction. Significant unloading of the target plates is predicted by radiation losses of C impurities [13].

The losses of fast ions (65 keV deuterons, 3 MeV protons and 1 MeV tritons) and their deposition patterns on plasma facing components are studied. Most of the lost counter-injected deuterons which carry most of the lost energy hit the divertor target plates, while only a small fraction of particles [14] interacts with the other surfaces.
First attempts to analyse the complex boundary physics of W7-AS, the precedent device of W7-X, using the 3D plasma transport EMC3 (Edge Monte Carlo 3D) have been started with promising results [15]. The Greifswald stellarator physics group is progressing with the development of a 3-D plasma fluid model based on the W7-X topology where strong stochastic effects become important [16].

3.1 EMC3-EIRENE modelling

The EMC3 code solves a set of Braginskii's fluid equations in a 3D space with Monte Carlo technique. The Monte Carlo method allows a high flexibility in construction and distribution of the computational mesh for complex 3D structure of W7-X edge region. The Monte Carlo particles representing physical quantities such as mass, momentum and energy undergo convective and diffusive process in parallel and cross-field directions. The magnetic field vectors are defined everywhere using the 3D mesh which represents a set of flux tube that are subdivided into toroidal cells to score particles [17]. For the present application of EMC3 in W7-X, a constant in flux of energy entering the SOL region is used from the core region. The edge plasma density is fixed by the choice of total plasma flow to the targets while the volume sources are used as generated by EIRENE code. At the targets the Bohm boundary condition is used.
The code EMC3-EIRENE, recently upgraded to incorporate arbitrary magnetic structures, uses a 3D grid for sampling the plasma and neutral parameters. The signicantly large volume of W7-X plasma requires a proportionally large number of grid points for sampling plasma parameters since the required resolution is fixed by the scale lengths which are largely independent of the total plasma volume. The 3D divertor geometry also adds to the complexity of the analysis and requires a carefully chosen grid structure.
The 3D mesh used for simulation represents a set of flux tubes which are subdivided into toroidal cells to score particles. A finer cell size is required to resolve the region close to the divertor surfaces, where the neutral source is located and plasma parameters have the largest variation. This resolution is maintained on all toroidal locations on the 3D helical surface of the divertor plates. Apart from the finer geometric grid a coarser physical grid is used for defining physical variables.

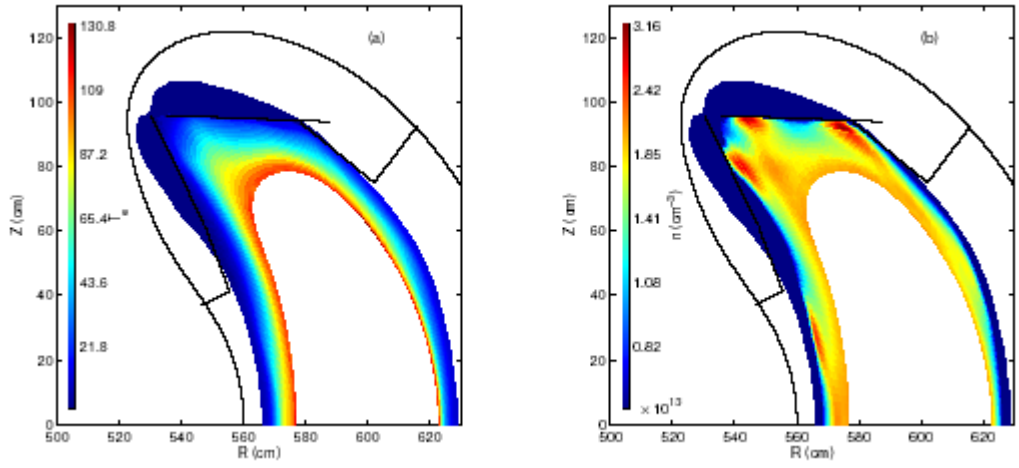

Fig.4: Electron temperature (T_e[eV]) and plasma density for the standard case with <β>=4% and 5 MW power flow across the separatrix in the poloidal plane corresponding to φ=0°.

The first application of EMC3-EIRENE [18] for the W7-X geometry is implemented. The plasma profiles are simulated self-consistently using an iterative procedure for the magnetic field configuration with ι = 5/5 and < β >= 4%.
The deposition channels to the target plates could be clearly identified as they follow the island structure (Fig. 4). The volume sources are seen to peak on the target surfaces with maximum value on the horizontal target plate close to the $\varphi = 0$ plane. In Fig. 5 the deposition pattern on the target area are presented for the standard case, <β> = 4% and an power flow of 5 MW. The upper part describes the pattern for the previous geometry "Target 2002", for comparison the recently modified version "Target +1°" with an increase of the angle of incidence by +1° is shown on the lower part. The reduced interaction area leads to a slight increase of the local power load as indicated by the colour bars (units of P/A [MW/m^2]).

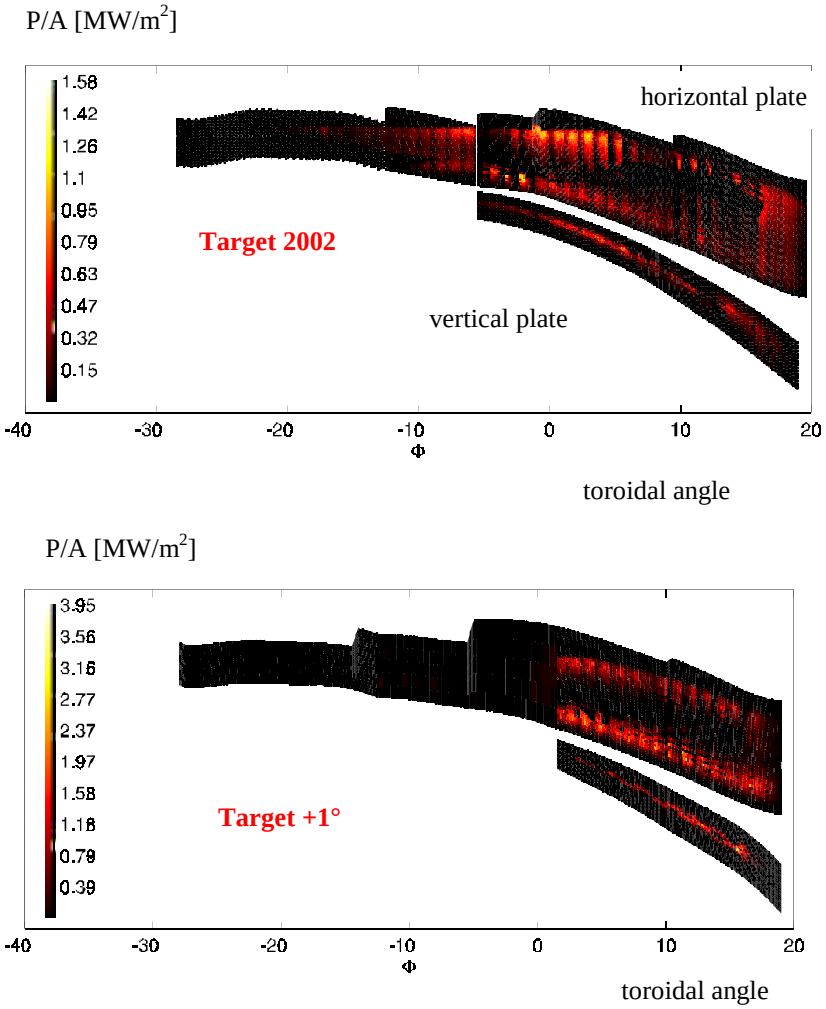

Fig.5 EMC 3studies: Deposition patterns on the target area of one divertor unit for the standard case and <β> =4%. (toroidal angle versus poloidal extension). Power flow: 5 MW. Upper part related to the previous geometry" Target 2002". The lower part presents the modified geometry "Target +1°". Note, the significant reduction of the interaction area and the increase of the local power deposition for the modified geometry.

4. DIVERTOR DESIGN

4.1 Energy exhaust

The components, related to the divertor units of W7-X are: the **P**lasma **F**acing **C**omponents: targets, baffles, wall protection [19], the pumping system, including cryopanels , control coils. The "open divertor" system for stationary operation with an input power of 10 MW is designed . As plasma facing material C, CFC, B_4C, low Z material will be used. A reduction of the expensive high heat load area was achieved by the increase of the inclination of the target areas by 1° versus the boundary flux bundles. The use of SepCarb NB31 as CFC material in combination with CuCrZr as heat sink has improved the heat removal capabilities

of the target elements. The concentration of the power deposition is illustrated in Fig. 6. Three loading areas with different heat load can be identified (Tab. 1).

		PFC material	**area**	**specified load**
divertor				
	target plates	**NB 31**	20 m²	10-12 MW/m²
			10 m²	< 1MW/m²
	baffle plates	**fine grain graphite**	32 m²	0.5 MW/m²
	wall		115 m²	
		Inboard: graphite tiles	45 m²	250/(500) kW/m²
		out board: SS panels, B_4C coated	70 m²	200 kW/m²

Table 1: Specifications of the plasma facing area inside the plasma vessel

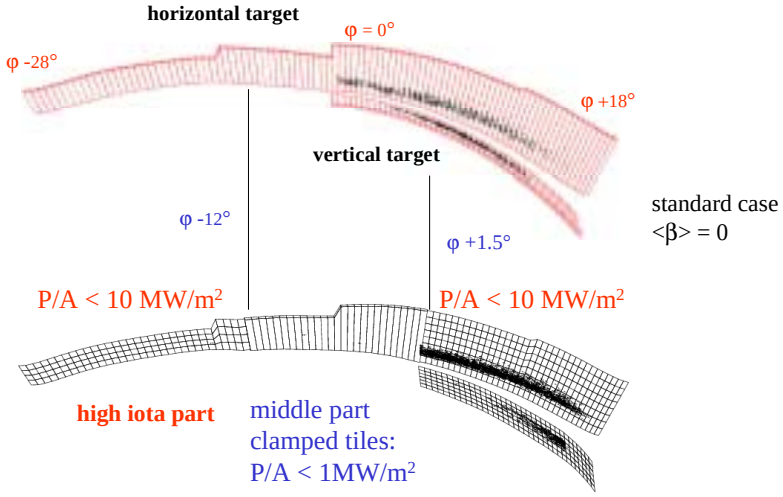

Fig.6: "Field line tracing" Deposition pattern for the standard case before (upper part) and after modification of the target geometry (inclination by +1°):The concentration of the deposition pattern allows a reduced specification of the area between the toroidal angle –12° to +1.5° (lower part).

4.2 Particle exhaust

To achieve efficient pumping baffle plates have been introduced to concentrate the recycling neutral particles close to the target and pumping gap between the target plates of the divertor units. The optimisation of the geometry was based on 3D EIRENE [20] studies. Recently the chosen geometry of the pumping gap was verified by results of EMC3 studies [18]. Including cryo-panels and TM-pumps a total pumping speed of 150,000 l/s will be provided [21].
Maximum fluxes up to 10^{23} electron-ion-pairs/s associated with the convective power source of 10 MW are estimated at the targets with temperatures less than 10 eV. The particle flow across the LCMS which depends on the density range and the confinement is estimated to be several 10^{22} particles/s. External fluxes by NBI, localised gas puffing and pellet injection in a range up to 10^{22} particles/s will be applied [22].

5. CONCLUSIONS

The stellarator Wendelstein 7-X is designed for steady-state operation. Within a wide range of magnetic parameters and applying different heating scenarios with possibilities of current drive, gas feed, pellet injection the optimised properties of the HELIAS configuration will be proven. The properties of the magnetic configuration allow to select a divertor geometry

without needs of adjustment dependent of the particular plasma parameters and <ß>. The adaptation for a wide operational range of the magnetic parameters requests an "open divertor". Additionally, experimental flexibility is provided by means of control coils.
The approach on the basis of the Monte-Carlo EMC 3 code which has been developed for W7-AS and recently applied for divertor experiments is very promising. First results of the EMC 3 code studies of the W7-X boundary are in fair agreement with previous more simplified investigations for the design. Supplementary to the EMC 3 code, a multi-fluid model for 3D geometry is in progress.
Depending on the improvement of understanding and modelling of the 3D boundary plasma some changes of the geometry and specifications have to be expected until the start of the experiment, planned on 2010.

REFERENCES

[1] G. Grieger, W. Lotz, P. Merkel, J. Nührenberg, J. Sapper, E. Strumberger et al., "Physics Optimization of Stellarators", *Physics of Fluids*, B4 (1992), 2081 - 2091
[2] J. Nührenberg and R. Zille, *Phys. Lett.*, 114A, 129 (1986).
[3] J. Nührenberg and R. Zille, *Phys. Lett.*, 129A, 113 (1988).
[4] H. Renner et al., Nucl .Fusion 40(2000), p 1083-1093
[5] H.Renner et al., IAEA Lyon (2002)
[6] J. Kisslinger, T. Andreeva Internal Report, IPP (2003)
[7] R. Schneider et al., Plasma Phys. Control. Fusion, 44 (2002), 665-672
[8] E. Strumberger, Nucl. Fusion 36 (1996), p. 891-908
[9] E. Strumberger, IPP-report 2/339 (1997)
[10] E. Strumberger, Nucl. Fusion 37 (1997), p.19 – 27
[11] E. Strumberger, Contr. Plasma Phys. 38 (1998), p. 106
[12] B.J. Braams, Ph.D. Thesis, Rijksuniversiteit Utrecht (1984)
[13] H. Renner et al., J. Nucl. Mater. 241-243 (1997), p. 946-449
[14] E. Strumberger, Nucl. Fusion 40 (2000), p. 1697-1713
[15] F. Sardei et al., J. Nucl. Mater. 241-243 (1997), p. 135-148
[16] M. Borchardt et al., J. Nucl. Mater. 290-293 (2001), 546-550
[17] Y. Feng, F. Sardei, J. Kisslinger, J. Nucl. Mater. 266-269 (1999) 812-818
[18] D. Sharma et al., EPS St. Petersburg (2003), P1.14
[19] H. Greuner et al., SOFT Helsinki (2002)
[20] D. Reiter, Jülich Report 1947, Jülich (1984)
[21] H. Grote et al., this workshop
[22] H. Grote et al., J. Nucl. Mater. 313-316 (2003) 1298-1303